JPE 18-5-7

https://doi.org/10.6113/JPE.2018.18.5.1357
ISSN(Print): 1598-2092 / ISSN(Online): 2093-4718

# Non-Isolated High Gain Bidirectional Modular DC-DC Converter with Unipolar and Bipolar Structure for DC Networks Interconnections

Lejia Sun*, Fang Zhuo*, Feng Wang†, and Hao Yi*

†,*School of Electrical Engineering, Xi'an Jiaotong University, Xi'an, China

**Abstract**

In this paper, a novel high gain bidirectional modular dc-dc converter (BMC) with unipolar and bipolar structures for dc network interconnections is proposed. When compared with traditional dc grid-connecting converters, the proposed converter can achieve a high voltage gain with a simple modular transformerless structure. A sub-modular structure for the BMC is proposed to eliminate the unbalanced current stress between the different power units (levels) in the BMC. This can realize current sharing and standardized production and assembling. In addition, phase-interval operation is introduced to the sub-modules to realize low voltage and current ripple in both sides of the converter. Furthermore, two types of bipolar topologies of the sub-modular BMC were proposed to extend its application in bipolar dc network connections. In addition, the control system was optimized for grid-connection applications by providing various control strategies. Finally, simulations of a 3-level unipolar sub-modular BMC and a 4-level bipolar sub-modular BMC were conducted, and a 1-kW experimental 3-level unipolar prototype was developed to verify the effectiveness of the proposed converter.

**Key words:** Current control, DC-DC power conversion, Grid connection, Pulse width modulation

## I. INTRODUCTION

In the past few years, high-voltage dc (HVDC) transmission has become a mature technology for efficiently transferring large amounts of energy across large distances [1], [2]. In addition, the increasing amount of renewable energy has stimulated dc transmission technology extending to the lower voltage area [3], [4]. It has been shown that renewable energy sources such as windfarms and photovoltaic (PV) power plants operate more efficiently when they are connected to a dc networks instead of an ac grid [5], [6]. Furthermore, storage systems are essential for leveling out the volatility of supplies. These storage systems, e.g. battery storage systems, are dc sources. Renewable energy sources and storage systems with lower voltage levels need to be integrated efficiently using high voltage gain dc-dc converters, which is highlighted in Fig. 1.

Manuscript received Dec. 12, 2017; accepted May 19, 2018
Recommended for publication by Associate Editor Younghoon Cho.
†Corresponding Author: fengwangee@mail.xjtu.edu.cn
Tel: +8615829389307, Xi'an Jiaotong University
*School of Electrical Eng., Xi'an Jiaotong University, China

Generally, high voltage gain DC-DC converters are divided into two categories: isolated and non-isolated. Recently, a considerable amount of attention has been paid to isolated high voltage gain DC-DC converters. Researchers have proposed the dual-active bridge (DAB) converter and the face-to-face modular multilevel converter (MMC), both of which were widely used in HVDC or MVDC systems. However, the DAB converter has serious drawbacks, such as a high circulating current and a high voltage stress across the output diodes that is larger than the output voltage. In addition, its efficiency is greatly reduced when the output voltage is high [7]. The MMC involves one huge, high-power, three-phase transformer for voltage conversion. The required transformer with its high isolation and high frequency is difficult to manufacture and continues to face some technical bottlenecks. Furthermore, the weight, parasitics, losses and cost associated with thes e transformers add to the system complexity.

In applications in which galvanic insulation is not required, non-isolated DC-DC topologies are suitable choices to achieve a high voltage gain. The consequent reduction of size, weight

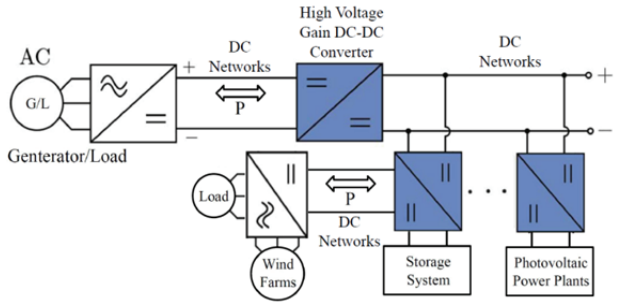


Fig. 1. Simplified block diagram of a future dc network.

and volume is associated to improved efficiency due to the lack of a high-frequency transformer [8]. A basic buck-boost con verter is recommended due to its low power level and simple structure. However, in practice, basic buck-boost converters suffer from problems of low efficiency in terms of switch utilization and high voltage stress on the switching devices, which limit its voltage gain [9], [10].

In order to overcome these drawbacks, some other non-isolated high gain DC-DC converters based on basic buck-boost converters have been developed, such as the cascaded DC-DC converter and the interleaved DC-DC converter. In the cascaded DC-DC converter, a wide conversion ratio, high switch utilization and reduced current ripple can be achieved if two or more conventional buck-boost converters are cascaded [11], [12]. However, its robustness is compromised since the converter needs multiple active switches, diodes, inductors and capacitors with no voltage stress reduction, which limits its application in high-voltage fields. Furthermore, its output power is limited by its cascaded structure.

The interleaved dc-dc converters in [13], [14] are commonly used in high power applications and efforts have been made to further reduce the input current ripple of these converters in [15]-[18]. However, the main drawback of these converters lies in the presence of an auxiliary transformer used to achieve a high voltage gain. In addition, a common fatal flaw of the cascaded DC-DC converters and interleaved DC-DC converters is the high voltage stress across the switches, which limits their voltage level and voltage gain expansion in industry applications.

In order to solve these problems, a high step-up DC-DC converter based on a coupled-inductor with a modularized structure was proposed in [19]. The converter consists of a synchronous rectification boost unit and multiple coupled-inductor-SC (CLSC) units, which can be added to extend the voltage gain. However, due to the voltage gain increase, the top-level CLSC unit requires an extra high isolation transformer which is difficult to manufacture and limits the extension of its voltage gain. Furthermore, the weight, parasitics, losses and cost associated with the transformers increase the system complexity.

With the increasing complexity of DC networks, the power should be transmitted in multiple directions. However, most

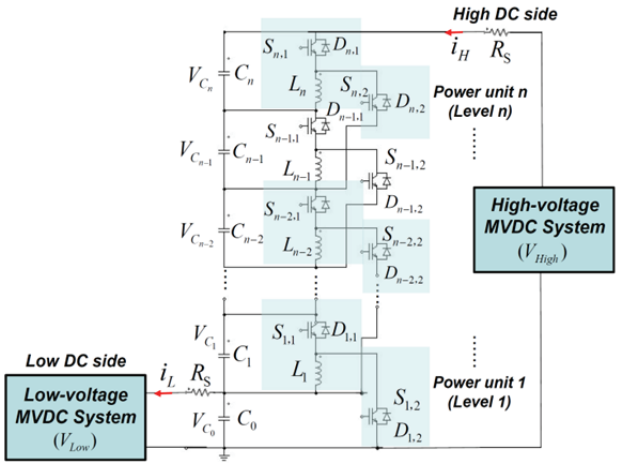


Fig. 2. Unipolar BMC with n resonant power units.

of the converters mentioned above cannot meet the requirements of power interaction since they are all unidirectional converters and can only connect between dc networks with unidirectional power transmission. In order to realize bidirectional power interaction, another kind of bidirectional high gain modular dc-dc converter, the multilevel modular capacitor-clamped converter (MMCCC), was proposed in [20]-[24]. The MMCCC is widely used in hybrid electric and fuel cell automobile power supply systems. However, it still has some inherent disadvantages when used in dc network connections. Firstly, it requires a large number of switches, which greatly increases the switching loss, control complexity and cost. Secondly, high-current pulses occur because two capacitors with different voltages are connected in parallel at each switching instant. This can restrict the power level to which a MMCCC can be applied. Thirdly, an unbalanced voltage occurs among the capacitors. The capacitors near the high voltage side have a higher voltage stress than the capacitors near the low voltage side. This can lead to a huge size of the high voltage capacitor, since with the same capacitance, when the voltage stress of the capacitor is doubled, the volume of the capacitor is increased by 4 times. Finally, the MMCCC can only be applied in unipolar dc networks due to its unipolar structure. In addition, it cannot be connected between bipolar dc networks which have been widely adopted by the practical dc networks power systems.

In this paper, a novel unipolar bidirectional modular dc–dc converter (BMC) for dc networks connection is introduced in section II, as is shown in Fig. 2. The BMC consists of a string of series capacitors and several power units (levels). It has the following merits:

(1) A high voltage gain achieved with a simple, modular and transformerless structure.

(2) Voltage sharing realized between the capacitors.

(3) Easy expansion of the voltage gain by employing multiple resonant power units.

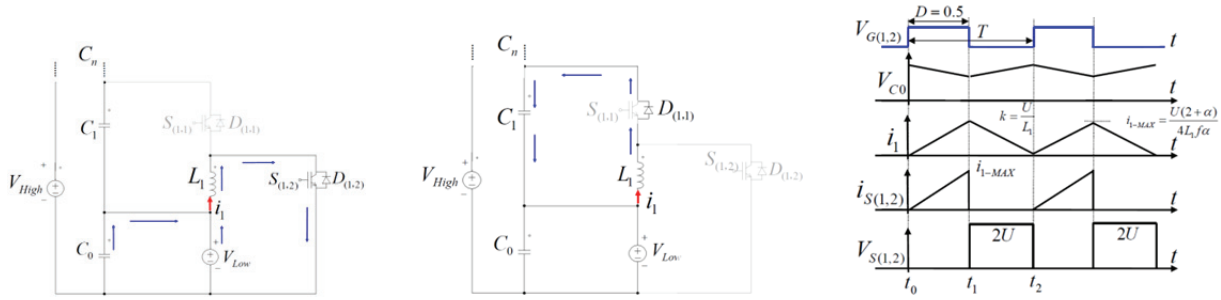


(a) (b) (c)

Fig. 3. Transfer process of the unipolar BMC with $n$ power units in the boost mode when power is transferred from $C_L$ to $C_1$: (a) Operation state: *Stage I* ($t_0$–$t_1$), (b) Operation state: *Stage II* ($t_1$–$t_2$), (c) Theoretical waveform in boost mode.

TABLE I
COMPARISON BETWEEN A MMCCC AND THE PROPOSED CONVERTER

| | Module number | Switch number | Bi-direction | Bipolar structure | Voltage sharing | Auxiliary transformer | Precise power control |
|---|---|---|---|---|---|---|---|
| MMCCC in [20] | 9 | 28 | Yes | No | No | No | No |
| Proposed unipolar BMC | 9 | 18 | Yes | Yes | Yes | No | Yes |

Based on the assumption that the voltage gain is selected as 10, a comparison between the MMCCC in [20] and the proposed unipolar BMC is summarized in Table I.

In section III, the sub-modular structure of the BMC is proposed to solve the eliminate the current stress between different power units in the BMC. In the sub-modular BMC, each power unit can be further modularized into several sub-modules to realize current sharing. In section IV, based on the sub-modular structure, two types of bipolar sub-modular BMCs are introduced to extend its application in bipolar dc networks connection.

Compared with the former unipolar BMC, the bipolar sub-modular BMC has the following additional advantages:

(1) Standardized production and assembling achieved by the sub-modules that share the same component parameters.

(2) Small input and output ripple due to the sub-modules working in phase-interval operation.

(3) Interconnection capability between unipolar and bipolar dc networks.

(4) Flexible control strategies of the grid-connection achieved by the proposed localized sub-modules PWM control system, which is illustrated in detail in section V.

## II. OPERATION PRINCIPLE OF THE UNIPOLAR BMC

### A. Operation Principle

The unipolar BMC converter is shown in Fig. 2. Each of the power units, which can also be called levels, includes two switching devices $S_{n,1}$ and $S_{n,2}$, and one inductor $L_n$. For a certain power flow direction, one of the switches is used as a power switch and the other is used as a freewheeling diode. By utilizing the L-C resonance of the power unit to transmit power and to maintain the voltage balance among the series capacitors, the BMC can achieve a high gain between the voltage of the capacitors in series and the voltage of the bottom-level capacitor. The unipolar BMC has two operation modes: the buck mode and the boost mode. The working principles are explained based on the following assumptions:

1) The voltage for all of the power units is equal (i.e., $V_{C0} = V_{C1} = V_{C2} = \ldots = V_{Cn} = U$).

2) All of the components are analyzed in ideal models.

3) To simplify the analysis, the power unit is assumed to be operating at the CCM/DCM boundary at a full load.

To aid with visualization and understanding, only the power transfer process between the top two adjacent power units in the buck mode and the bottom two adjacent power units in the boost mode was selected for analysis. However, this discussion is suitable for all of the other adjacent power units.

In the boost mode, the power flow of the converter is from the low-voltage dc source $V_{Low}$ to the high-voltage dc source $V_{High}$. The power unit can pump power from the capacitor $C_0$ to the capacitor $C_n$ step by step. In addition, it can keep the voltage of all the series capacitors as $U$. Fig. 3(c) shows a theoretical waveform when the power is pumped from the capacitor $C_0$ to the capacitor $C_1$. This power transferring process can be divided into two stages. These are illustrated separately in Figs. 3(a) and 3(b). $V_{G(1,2)}$ is the driving signal of $S_{1,2}$. $f$ is the switching frequency. $i_{1\text{-}MAX}$ is the maximum value of the inductor current of the power unit.

***Stage I ($t_0$–$t_1$):*** At $t_0$, $S_{1,2}$ is turned on, $S_{1,1}$ is turned off, and power is transferred from $C_0$ to $L_1$. At the same time, the voltage $V_{C0}$ is reduced and the current $i_1$ increases. The rated voltage of $S_{1,1}$ is the sum of $V_{C0}$ and $V_{C1}$, which is $2U$. $k$ is the increasing gradient of $i_1$, and $i_{1\text{-}MAX}$ is the maximum value of $i_1$, which are calculated as:

$$k = \frac{di_1}{dt} = \frac{U}{L_1}, \tag{1}$$

$$i_{1-MAX} = \frac{U}{2L_1 f\alpha}\left(1+\frac{\alpha}{2}\right). \tag{2}$$

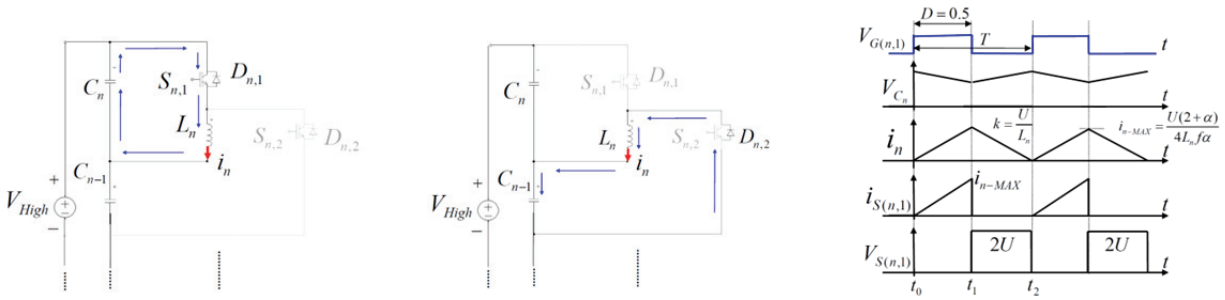


(a) (b) (c)

Fig. 4. Transfer process of the unipolar BMC with $n$ power units in the buck mode when power is transferred from $C_n$ to $C_{n-1}$: (a) Operation state: *Stage I ($t_0$–$t_1$)*, (b) Operation state: *Stage II ($t_1$–$t_2$),* (c) Theoretical waveform in buck mode.

***Stage II ($t_1$–$t_2$):*** At $t_1$, $S_{1,2}$ is turned off. The current $i_1$ continuously flows through the antiparallel diode $D_{1,1}$, and power is transferred from $L_1$ to $C_1$. Then $i_1$ declines and $V_{C1}$ increases. The voltage $V_{C0}$ is recovered by the charging of the input voltage $V_{Low}$. The rated voltage of $S_{1,2}$ is the sum of $V_{CL}$ and $V_{C1}$, which is $2U$. The declining gradient of $i_1$ is also equal to $k$.

Then at $t_2$, $S_{1,2}$ is turned on again, and the following processes are circulated to Stage I.

When the converter operates in the buck mode, the power flow is reversed. Fig. 4(c) shows theoretical waveforms when the power is transferred from the capacitor $C_n$ to the capacitor $C_{n-1}$, and the power transfer process can also be divided into two stages, which are illustrated separately in Figs. 4(a) and 4(b).

### *B. Unbalance Current and Asymmetrical Parameters*

In a unipolar BMC with $n$ power units, the voltage gain N can be achieved as $N=V_{High}/V_{Low}=n+1$. The power transferred by the $n$-th power unit can be expressed by $(N-n)P/N$, where $i_k$ is the inductor current in the $k$-*th* power unit. The following mathematical relations can be deduced:

$$L_k \cdot \frac{di_k}{dt} = U, \tag{3}$$

$$t_{on} = \frac{D}{f}, \tag{4}$$

Where $f$ represents the switching frequency, and $D$ represents the duty cycle. From (3) and (4), the maximum inductor current $i_{k\text{-}MAX}$ can be obtained by:

$$i_{k-MAX} = \frac{UD}{L_k f}. \tag{5}$$

Because the inductor current increases from zero, $\Delta i_k = i_{k\text{-}MAX}$. To maintain the energy balance of the inductor $L_k$, the following equation can be used:

$$\frac{N-k}{N} \cdot P = \frac{1}{2} \cdot L_k \cdot f \cdot i_{k-MAX}^2. \tag{6}$$

From (5) and (6), the inductance $L_k$ can be expressed as:

$$L_k = \frac{NU^2D^2}{2fP(N-k)} \tag{7}$$

If $L_k$ is selected based on $D_{MAX} = 0.5$, then:

$$L_k = \frac{NU^2}{8fP(N-k)} \tag{8}$$

Based on (6), different power units transfer different amounts of power between adjacent capacitors. Furthermore, as can be seen from (5) and (7), a step by step reduction in the inductor current of the power units from $i_1$ to $i_n$ and can result in different inductance values $L_k$ and other asymmetrical parameters between the power units. This can make a modular converter difficult to design.

## III. SUB-MODULARIZATION OF UNIPOLAR BMC

### *A. Sub-Modular Structure*

To solve the unbalanced current and asymmetrical parameters problems mentioned above, a sub-modular structure of the BMC was proposed, as shown in Fig. 5. Each of the resonant power units has been divided into several paralleled sub-modules to share the inductor current. In an $n$-level (with n power units) unipolar sub-modular BMC, the number of sub-modules in the $k$-th level can be expressed as:

$$J_k = n - k + 1. \tag{9}$$

The total number of sub-modules ($Q_{sub}$) and switching devices ($Q_S$) can be expressed as:

$$Q_{sub} = \sum_{k=1}^{n} J_k = \frac{(n+1)n}{2} \tag{10}$$

$$Q_S = 2Q_{sub} = n(n+1). \tag{11}$$

### *B. Phase-Interval Operation*

As can be seen in the theoretical waveforms of Fig. 3(c) and Fig. 4(c), there are large ripples in both the voltage and current of the power units (levels). With an increasing number of sub-modules and levels in a sub-modular BMC, the ripples become further aggravated and result in larger

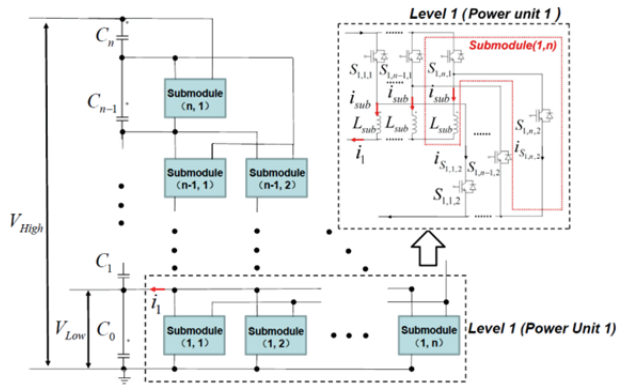


Fig. 5. Topology of an *n*-level unipolar sub-modular BMC.

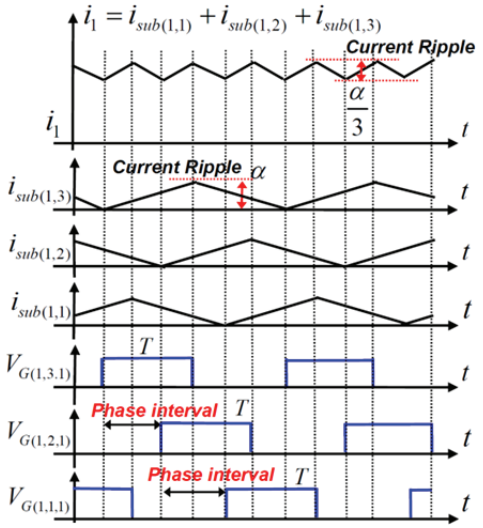


Fig. 6. Analysis of the current ripple reduction of a level with three sub-modules in phase-interval operation.

ripples at both sides of the converter. In this paper, a phase-interval operation for sub-modules is applied to reduce the current ripples and to improve the output quality. Since a localized control system is applied to the sub-modular BMC, each of the sub-modules has independent PWM control. The gating signals of the sub-modules at the same level can be set with an equal interval of a certain phase. In the *k*th-level, the interval phase of the *j*-th sub-module can be expressed as:

$$\delta_j = \frac{2\pi(j-1)}{n-k} \qquad 1 \le j \le n\text{-}k\text{+}1. \tag{12}$$

Fig. 6 illustrates current ripple reduction in a level with three sub-modules in phase-interval operation. For the non-phase-interval case, the current ripple of the level ($i_1$) is a factor of 3 higher than the current ripple of each submodule. In contrast, as can be seen in the figure, for the phase-interval case, the current ripple of the level ($i_1$) is a factor of 1/3 lower than the current ripple of the submodules. Therefore, the current ripple of the level in phase-interval operation is reduced by a factor of 9 when compared to that in non-phase-interval operation.

### C. Design of the Sub-module Inductor $L_{sub}$

The design of the submodule is based on its rated voltage $U$ and rated power $P_{sub}$. In addition, $\alpha$ is the ripple of sub-module current $i_{sub}$. Therefore, $i_{sub}$ can be expressed as:

$$i_{sub} = \frac{U}{2L_{sub} f\alpha}. \tag{13}$$

Maintaining an energy balance in a sub-module inductor $L_{sub}$ requires that:

$$P_{sub} = \frac{1}{2} \cdot L_{sub} \cdot f \cdot [(i_{sub} + \frac{\alpha}{2} i_{sub})^2 - (i_{sub} - \frac{\alpha}{2} i_{sub})^2] \tag{14}$$

From (13) and (14), $i_{sub}$ can be further expressed as:

$$i_{sub} = \frac{2P_{sub}}{U}. \tag{15}$$

From (13) and (15), $L_{sub}$ can be calculated as:

$$L_{sub} = \frac{U^2}{4f\alpha P_{sub}} \tag{16}$$

### D. Design of the capacitor $C_n$

Serial capacitors are an essential components of the sub-modular BMC for the transmission of energy. To easily maintain the voltage balance between series capacitors, they are selected to have the same capacitance. The voltage ripple $\beta$ of $C_0$ is expressed as:

$$\beta = \frac{\Delta V_{C0}}{V_{C0}} \tag{17}$$

Maintaining the energy balance in the capacitor $C_0$ requires that:

$$\frac{1}{2} \cdot C_0 \cdot [(U + \frac{\beta}{2} U)^2 - (U - \frac{\beta}{2} U)^2] \cdot f = \frac{(N-1) \cdot P}{N}. \tag{18}$$

From (17) and (18), the capacitance can be obtained as:

$$C_n = C_0 = \frac{P(N-1)}{Nf\beta U^2}. \tag{19}$$

## IV. Two Types of Bipolar BMCs

Generally speaking, bipolar dc transmission networks present clear advantages when compared to their unipolar counterparts, such as increased energy transmission capacity and higher reliability due to the possibility of power transfer when a line fails. In this section, two types of bipolar sub-modular BMCs are introduced.

The first type of bipolar sub-modular BMC to be proposed is referred to as unipole-to-bipole sub-modular BMC as shown in Fig. 7. This is for use in cases where a renewable energy system with a unipole and a low voltage level, such as the PV, fuel cell, and uninterruptible power supplies systems, needs to be connected with bipolar DC networks. In the unipole-to-bipole sub-modular BMC, the number of levels should be odd ($2n-1$). The part of the converter above level

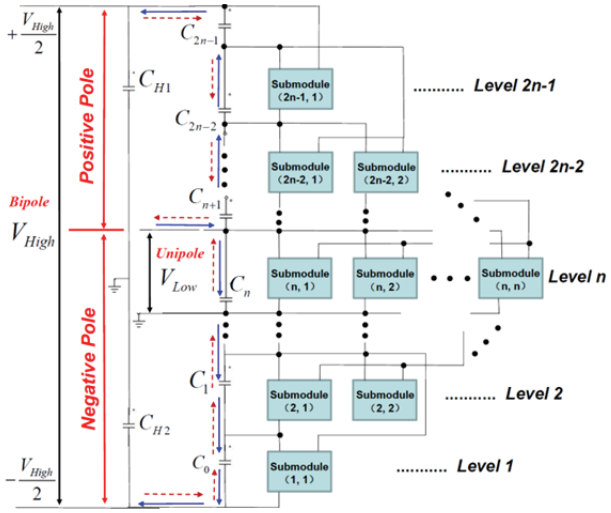


Fig. 7. Unipole–bipole sub-modular BMC.

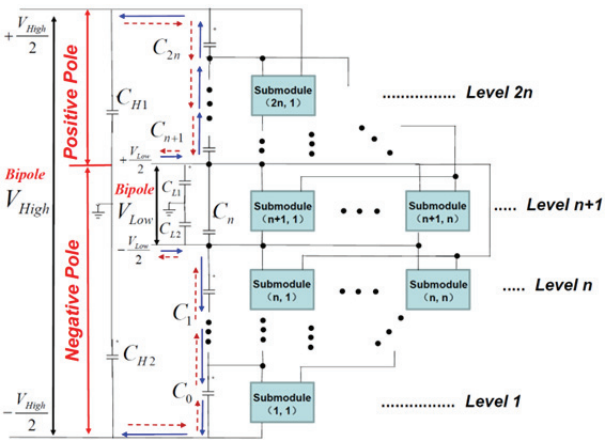


Fig. 8. Bipole–bipole sub-modular BMC.

TABLE II
OPERATION MODES OF A BIPOLAR SUB-MODULAR BMC

| Operation Mode | Positive Circuit | Negative Circuit |
|---|---|---|
| Up-conversion | in boost mode | in buck mode |
| Down-conversion | in buck mode | in boost mode |

(n)—that is, from level (n+1) to level (2n-1)—is referred to as the positive circuit, whereas the rest of the part is referred to as the negative circuit.

Second, when it is necessary to realize an interconnection between two bipolar DC networks, another type of bipolar sub-modular structure, the bipole-to-bipole sub-modular BMC, is applicable, as shown in Fig. 8. In a bipole-to-bipole sub-modular BMC, the part of the converter above level (n+1)—that is, from level (n+2) to level (2n)—is referred to as the positive circuit, whereas the rest of the part is referred to as the negative circuit.

According to the power flow direction, both types of bipolar converters have two operation modes: up-conversion and down-conversion. In each operation mode, both the positive and negative circuits can be considered as an independent unipolar sub-modular BMC, as shown in Fig. 5.

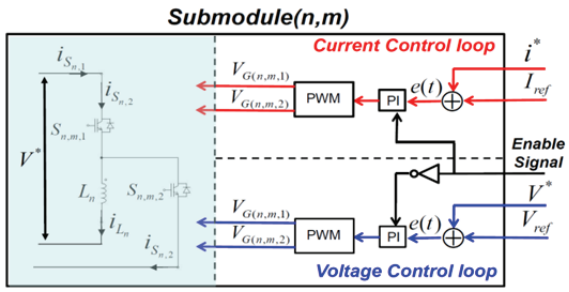


Fig. 9. Control block diagram of the sub-module controller.

When bipolar sub-modular BMCs work in the up-conversion mode, the positive circuit works in the boost mode and the negative circuit works in the buck mode. The power-transfer route is represented by the blue arrows in Fig. 7 and Fig. 8. The power is finally transferred to high-voltage dc networks and supports $\pm V_{High}/2$ with a stable output. When the bipolar converter works in the down-conversion mode, the power flow is reversed. The positive circuit works in the buck mode and the negative circuit works in the boost mode. The power-transfer route is represented by the red arrows in Fig. 7 and Fig. 8. Table II shows the operation mode characteristics of the positive circuit and the negative circuit in both of the bipolar sub-modular BMCs. The working principles of the positive and negative circuits have been presented in Section II.

## V. CONTROL SYSTEM

A precise control system is essential for grid-connecting converters. A localized control system is proposed in the sub-modular BMC to achieve a more flexible and precise control among dc networks systems. The control system consists of two levels: the central controller and the sub-module controller. The sub-module controller is the localized level integrated in each of the sub-modules as shown in Fig. 9. The sub-module controller can be switched between a current control loop and a voltage control loop by an enable signal, which includes the functions of receiving reference signals from the central controller, executing pulse-width-modulation (PWM) control of the sub-module, sampling and uploading voltage and current measurements to the central controller, and driving the switching devices. The central controller is the top level of the control system. It is responsible for enabling the current or voltage control loop of each sub-module controller depending on the different control strategies, calculating and providing references to the sub-module controllers, monitoring the overall operation status of the converter, and detecting and isolating broken sub-modules. The sub-modular BMC provides three control strategies: power control, output voltage control and voltage gain control. To aid in this explanation, a 3-level unipolar sub-modular BMC is presented as an example.

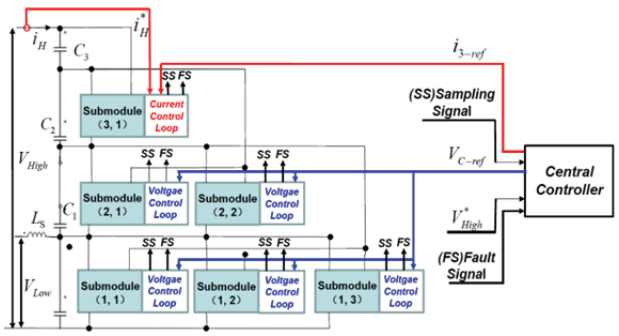


Fig. 10. Control block diagram of a 3-level unipolar sub-modular BMC in the buck mode with power control.

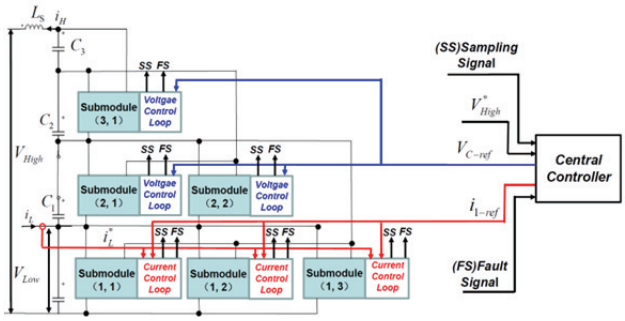


Fig. 11. Control block diagram of a 3-level unipolar sub-modular BMC in the boost mode with power control.

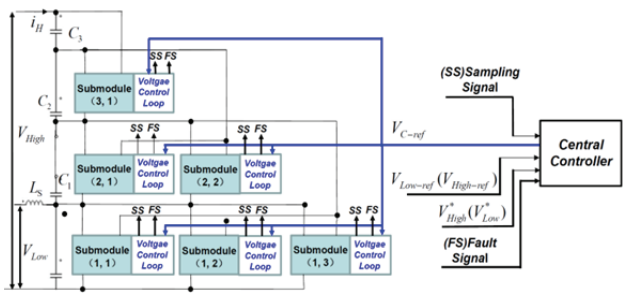


Fig. 12. Control block diagram of a 3-level unipolar sub-modular BMC with output voltage control.

### *A. Power Control*

The power control of a BMC is used in the following applications. 1. When a converter is required to connect with dc power systems such as battery storage systems, PV systems, or distributed generation systems to control the curve of its output power. 2. When a converter works as a grid converter to connect with dc networks and to perform precise power interaction. In the power control strategy, either the top-level sub-module controller or the bottom-level sub-module controller is set to the current control loops to achieve a constant power injection into the converter. The remaining sub-module controllers are set to voltage control loops.

A control block diagram of a 3-level unipolar sub-modular BMC with power control in the buck mode is shown in Fig. 10. In the buck mode, *Submodule Controller* (3,1) is set to the current control loop. The central controller measures the input voltage $V^*_{High}$ at each sampling period, and calculates the current reference $i_{3\text{-}ref}$ from:

$$i_{3-ref} = \frac{P_{ref}}{V^*_{High}}. \tag{20}$$

Then, *Submodule Controller* (3,1) receives $i_{3\text{-}ref}$ and maintains a constant power $P_{ref}$ output from the high-voltage dc system. The voltage control loop of the remaining submodule controllers guarantees that a constant power $P_{ref}$ is transferred from $C_3$ to $C_0$. When $C_0$ receives the power $P_{ref}$, a constant current $i_L$ flows to $V_{Low}$ through the filter inductor $L_S$. Then $i_L$ can be expressed as:

$$i_L = \frac{P_{ref}}{V_{Low}} \tag{21}$$

The voltage reference for the remaining sub-modules are given by:

$$V_{C-ref} = \frac{V^*_{High}}{n+1} = \frac{V^*_{High}}{4} \tag{22}$$

On the other hand, in the boost mode, *Submodule Controllers* (1,1), (1,2) and (1,3) are set to current control loops, while the remaining submodule controllers are set to voltage control loops. Its control block diagram is shown in Fig. 11. Like the principle of the power control in the buck mode, the remaining submodule controllers pump a constant input power $P_{ref}$ to $C_3$ and make the voltage of the series capacitors slightly higher than the high-voltage dc source ($V_{High}$). Then $P_{ref}$ is transferred to the high-voltage dc source through $L_S$. The current reference $i_{1\text{-}ref}$ for *Submodule Controllers* (1,1), (1,2) and (1,3) can be expressed as:

$$i_{1-ref} = \frac{P_{ref}}{V^*_{Low}}. \tag{23}$$

The voltage reference for the remaining submodules is given by:

$$V_{C-ref} = V^*_{Low}. \tag{24}$$

### *B. Output Voltage Control*

Output voltage control of a BMC is used in two different applications. 1. Applications where the converter needs to support the voltage of a dc networks. 2. Applications where a load is directly connected to the output. A control block diagram of a 3-level unipolar sub-modular BMC with output voltage control is shown in Fig. 12. In the output voltage control, all of the submodule controllers work in the voltage control loop to maintain their own voltage. The central controller measures the input voltage (i.e., $V^*_{High}$ or $V^*_{Low}$) at each sample period and calculates the reference voltage $V_{C\text{-}ref}$ for the submodule controllers. The voltage reference of each submodule controller in the boost mode is expressed as:

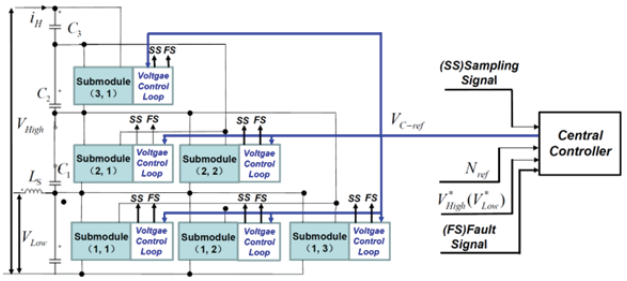


Fig. 13. Control block diagram of a 3-level unipolar sub-modular BMC with voltage gain control.

$$V_{C-ref} = (V_{High-ref} - V^*_{Low}) / n. \quad (25)$$

In the buck mode, it is expressed as:

$$V_{C-ref} = (V^*_{High} - V_{Low-ref}) / n. \quad (26)$$

### C. Voltage Gain Control

When the converter works as a dc–dc transformer, the voltage gain is required to maintain a constant value between two dc networks. A control block diagram of a 3-level unipolar sub-modular BMC with voltage gain control is shown in Fig. 13. The central controller samples the input voltage (i.e., $V^*_{High}$ or $V^*_{Low}$) and calculates the voltage reference $V_{C\text{-}ref}$ for each of the submodule controllers based on the constant conversion ratio $N_{ref}$ and the number of levels $n$. All of the submodule controllers receive $V_{C\text{-}ref}$ and work in a voltage control loop.

In the buck mode, the voltage reference for each of the submodule controllers is expressed as:

$$V_{C-ref} = \frac{N_{ref} \cdot V^*_{High} - V^*_{High}}{nN_{ref}}. \quad (27)$$

In the boost mode, the voltage reference for each of the submodule controllers can be expressed as:

$$V_{C-ref} = \frac{N_{ref} \cdot V^*_{Low} - V^*_{Low}}{n}. \quad (28)$$

## VI. Simulation Results

### A. Simulation of a Sub-modular BMC with Output Voltage Control

To verify the feasibility of the output voltage control and voltage gain control, a simulation model of a 3-level unipolar sub-modular BMC has been established on PSIM simulation software with the following simulation parameters: $V_{high}$ = 4 kV, $V_{Low}$ = 1 kV, $f$ = 20 kHz, $P$ = 1 MW, $N$ = 4, $C_n$($n$ = 0,1,2,3) = 1 mF, and $L_{n,m}$($n$,$m$ = 1,2,3) = 50 uH.

Fig. 14 shows a simulation waveform of the converter in the boost mode with the output voltage control ($V_{in}$ = $V_{Low}$ = 1 kV and $V_o$ = $V_{high}$ = 4 kV). It can be seen that an equal voltage is realized between the capacitors ($V_{C1}$ = $V_{C2}$) and

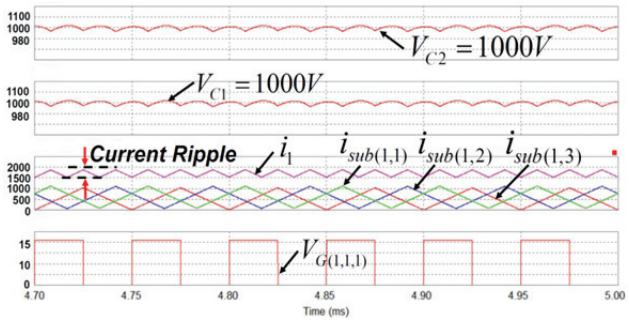


Fig. 14. Simulation of a 3-level unipolar sub-modular BMC in the boost mode with output voltage control ($V_{Low}$ =1 kV, $V_{High}$ = 4 kV).

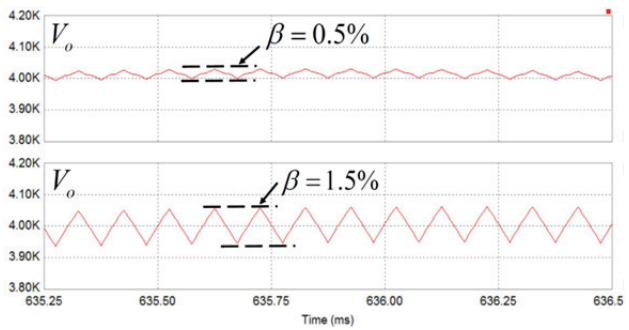


Fig. 15. Simulated output voltage ripple comparison between the non-phase-interval and phase-interval operation.

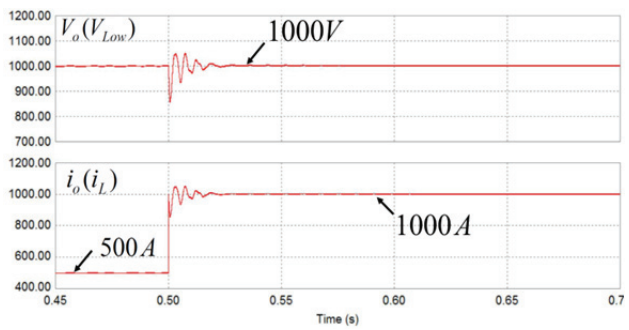


Fig. 16. Simulation of an output waveform of a 3-level unipolar sub-modular BMC in the buck mode with $P_{ref}$ stepped from 500 kW to 1 MW ($V_{High}$ = 4 kV and $V_{Low}$= 1 kV).

that current sharing is realized among the submodules ($i_{sub(1,1)}$ = $i_{sub(1,2)}$ = $i_{sub(1,3)}$). Fig. 15 shows a ripple comparison of the output voltage in the phase-interval operation and non-phase-interval operation. For the non-phase-interval case, the ripple of the output voltage is displayed as 1.5%. On the other hand, for the phase-shifted operation case, the ripple is reduced to 0.5%.

### B. Simulation of a Sub-modular BMC with Power Control

The dynamic step response is investigated in a simulation of a unipolar sub-modular BMC with power control. Fig. 16 shows an output waveform of a 3-level sub-modular unipolar BMC in the buck mode with a sudden change in the power

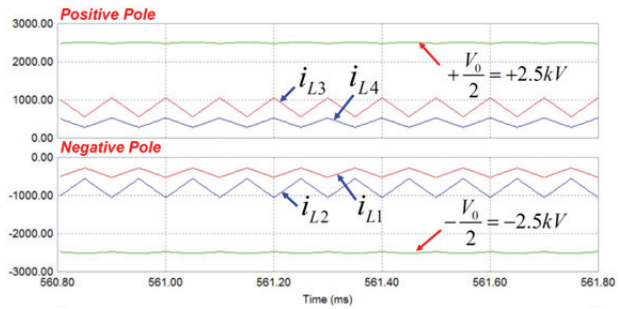


Fig. 17. Simulation of a 4-level bipolar sub-modular BMC with power control in the up-conversion mode.

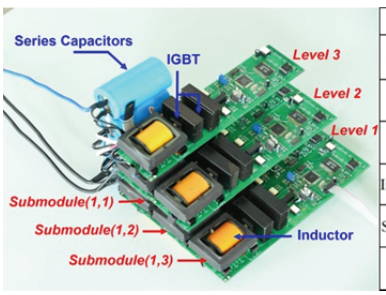


| Parameters | Value |
|---|---|
| Number of Levels | n=3 |
| Total Number of Submodule | $Q_{sub}$=6 |
| Rated Power | P=1kW |
| Input /Output Voltage | 100V/400V |
| Switching Frequency | $f$=20kHz |
| IGBT Mode | F912-11N120CND |

Fig. 18. Photograph of the 1-kW three-level prototype.

reference from 500 kW to the rated power of 1 MW. It should be noted that a slightly lower damping is observed during the transient process.

Fig. 17 shows waveforms of a 4-level bipolar sub-modular BMC with power control in the up-conversion mode ($\pm V_{in}/2 = \pm V_{Low}/2 = \pm 500$ V, $\pm V_O/2 = \pm V_{High}/2 = 2.5$ kV, and $P_{ref} = 1$ MW). When compared with the outcomes of Fig. 12, the inductor current level and its ripple are greatly reduced.

## VII. Experimental Results

Due to limited laboratory conditions, a small-scale (1-kW) 3-level prototype of a unipolar sub-modular BMC was developed, as shown in Fig. 18. The prototype was tested in the boost mode with power control. Fig. 19 shows current waveforms of the sub-modules in different levels to verify the current sharing between levels. Fig. 20 shows current waveforms of the sub-modules in the first level with the phase-interval operation. As expected, current sharing is achieved between the sub-modules in the first level, and the current ripple in this level is reduced to 1/3 of the current ripple in each of the sub-modules, which coincides with the theoretical and simulation result mentioned above. Fig. 21 shows the voltages for each of the series capacitors, which are stable at their reference value (100V). In addition, the output voltage reaches 400V. Furthermore, voltage waveforms of the switches $S_{(1,1,1)}$ and $S_{(1,1,2)}$ are plotted in Fig. 22. Fig. 23 shows the converter's dynamic step response during output power stepping from 250 W to 1 kW. A slightly lower damping is noted in the experimental system, and the output voltage is recovered within 2.5 ms.

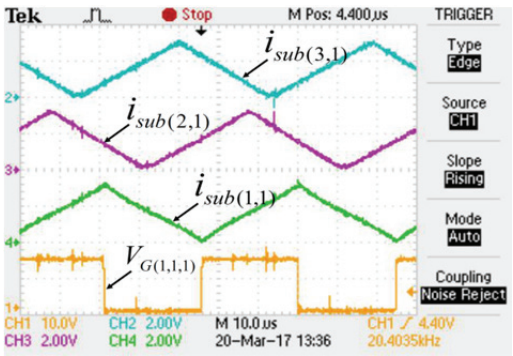


Fig. 19. Inductor current waveform of submodules in different levels (2.5 A/1 V).

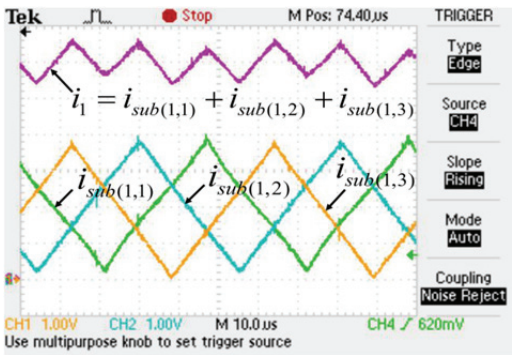


Fig. 20. Inductor current waveform of submodules in the first level (2.5 A/1 V).

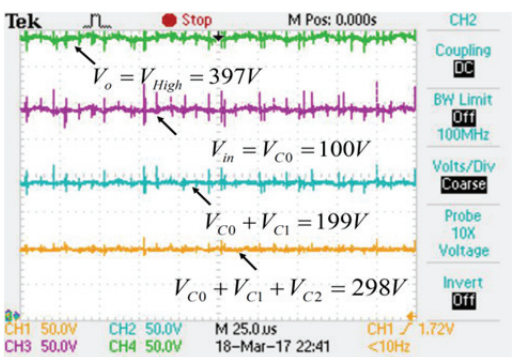


Fig. 21. Waveform of the voltage of series capacitors and output voltage $V_{High.}$

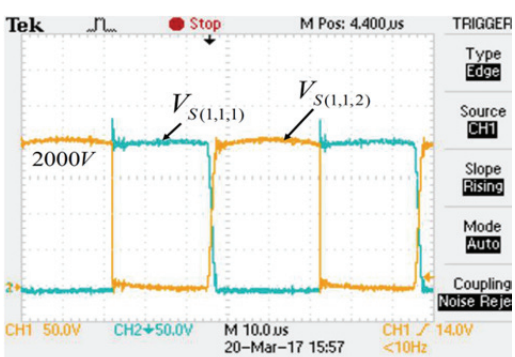


Fig. 22. Waveforms of switch voltage ($V_{S(1,1,1)}$ and $V_{S(1,1,1)}$).

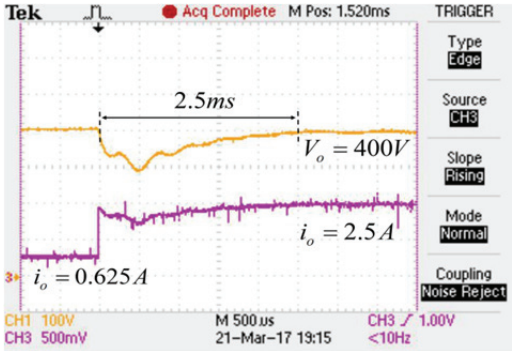


Fig. 23. Dynamic step response with the power stepped from 250W to 1kW.

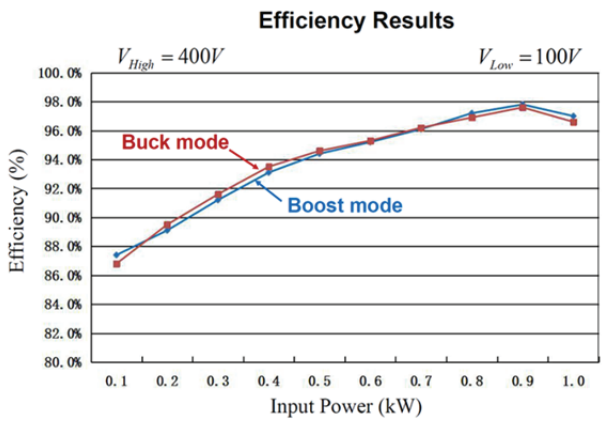


Fig. 24. Experimental efficiency of the prototype with power variations.

TABLE III
EFFICIENCY OF THE PROTOTYPE WITH DIFFERENT INPUT POWERS

| Output Power (kW) | In buck mode | In boost mode |
|---|---|---|
| P = 0.1 | 86.8% | 87.4% |
| P = 0.2 | 89.5% | 89.1% |
| P = 0.3 | 91.6% | 91.2% |
| P = 0.4 | 93.5% | 93.1% |
| P = 0.5 | 94.6% | 94.4% |
| P = 0.6 | 95.3% | 95.2% |
| P = 0.7 | 96.2% | 96.1% |
| P = 0.8 | 96.9% | 97.2% |
| P = 0.9 | 97.6% | 97.8% |
| P = 1.0 | 96.8% | 97.1% |

Table III and Fig. 24 show the measured efficiency of the prototype. The power conversion efficiency of the prototype was measured at input power levels ranging from 0.1 kW to 1 kW in both the boost and buck modes, with both efficiencies having very close values. It can be concluded that efficiency is not sensitive to power flow direction and that the slight difference between the boost and buck modes is mainly due to a slight difference in the electrical specifications between the switching devices and the layout of the printed circuit board (PCB) in the practical experimental prototype. The efficiency was measured at input power levels ranging from 0.1 to 1 kW. Maximum efficiencies of 97.8% and 97.6% were achieved for the boost and buck modes, respectively, at an input power of $P_{in}$ = 0.9kW. An efficiency up to 96% was achieved for a wide power range, and the efficiency at the rated power was about 97%.

## VIII. CONCLUSIONS

In this paper, a non-isolated bidirectional modular dc–dc converter based on a resonant power unit (BMC) with unipolar and bipolar structures for dc networks connection was introduced. In order to eliminate the unbalanced current stress between the different power units in the BMC, a sub-modular structure of the BMC is further proposed. When compared with traditional dc grid-connecting converters, the sub-modular BMC offers following improvements.

(1) High voltage gain achieved with a simple modular transformerless structure.
(2) Both voltage and current sharing are realized by its sub-modular structure.
(3) Easy expansion of the voltage gain and power capacity.
(4) Small input and output ripple achieved by the phase-interval operation.
(5) Interconnection capability between bipolar DC networks.
(6) Flexible control strategies optimized for grid-connection are achieved by the proposed localized sub-modules PWM control system.

Finally, a 1-kW implementation of the 3-level unipolar sub-modular BMC was developed. The obtained experimental results validate the operation principle and feasibility of the proposed converter.

## ACKNOWLEDGMENT

This paper was supported by National Key R&D Program of China (No. 2018YFB0904702 and No. 2018YFB0904600).

## REFERENCES

[1] G. J. Kish, and M. Ranjram, "A modular multilevel DC/DC converter with fault blocking capability for HVDC interconnects," *IEEE Trans. Power Electron.*, Vol. 30, No. 1, pp.148-162, Jan. 2015.
[2] D. Vinnikov, J. Laugis, and I. Galkin, "Middle-frequency isolation transformer design issues for the high-voltage DC/DC converter," in *2008 Power Electronics Specialists Conference,* pp. 1930-1936, 2008.
[3] S. Vighetti and J.-P. Ferrieux "Optimization and design of a cascaded DC/DC converter devoted to grid-connected photovoltaic systems," *IEEE Trans. Power Electron.*, Vol. 27, No. 4, pp. 2018-2027, Apr. 2012.
[4] R. Kadri and J.-P. Gaubert, "Nondissipative string current diverter for solving the cascaded DC–DC converter connection

problem in photovoltaic power generation system," *IEEE Trans. Power Electron.,* Vol. 27, No. 3, pp. 1249-1258, Mar. 2012.
[5] S. L Undberg, "Wind farm configuration and energy efficiency studies – Series dc versus ac layouts," *Ph.D. dissertation,* Chalmers University of Technology, Sweden, 2006.
[6] C. Meyer, "Key components f or future offshore dc grids," *Ph.D. dissertation, Inst. Power Generation and Storage Systems,* R W TH Aachen University, Aachen, Germany, 2007.
[7] Z. Chen, S. Liu, and L. Shi, "A soft switching full bridge converter with reduced parasitic oscillation in a wide load range," *IEEE Trans. Power Electron*., Vol. 29, No. 2, pp. 801-812, Feb. 2014.
[8] X. Hu, and C. Gong, "A high voltage gain dc–dc converter integrating coupled-inductor and diode–capacitor techniques," *IEEE Trans. Power Electron.,* Vol. 29, No. 2, pp. 789-800, Feb. 2014.
[9] F. S. Garcia, J. A. Pomilio, and G. Spiazzi, "Modeling and control design of the interleaved double dual boost converter," *IEEE Trans. Ind. Electron*., Vol. 60, No. 8, pp. 1292-1300, Aug. 2013.
[10] K. C. Tseng, C. C. Huang, and W. Y. Shih, "A high step-up converter with a voltage multiplier module for a photovoltaic system," *IEEE Trans. Power Electron*., Vol. 28, No. 6, pp. 3047-3057, Jun. 2013.
[11] L. Huber and M. M. Jovanovic, "A design approach for server power supplies for networking applications," *Proc. IEEE Applied Power Electronics Conf. And Exposition*, pp. 1163-1169, 2000.
[12] L. Huber and M. M. Jovanovic, "A design approach for server power supplies for networking applications," *Proc. IEEE Applied Power Electronics Conf. And Exposition*, pp. 1163-1169, 2000.
[13] M. S. Elmore, "Input current ripple cancellation in synchronized, parallel connected critically continuous boost converters," in *Proc. IEEE Appl. Power Electron. Conf.,* pp. 152-158, 1996.
[14] C. H. Chan and M. H. Pong, "Input current analysis of interleaved boost converters operating in discontinuous-inductor current mode," in *IEEE Power Electron. Spec. Conf.*, pp. 392-398, 1997.
[15] T. Ishii and Y. Mizutani, "Power factor correction using interleaving technique for critical mode switching converters," in *IEEE Power Electron. Spec. Conf.*, pp. 905-910, 1998.
[16] N. Genc and I. Iskender, "DSP-based current sharing of average current controlled two-cell interleaved boost PFC converter," *IET Power Electron.,* Vol. 4, No. 9, pp. 1015-1022, Nov. 2011.
[17] T. Nouri, S. H. Hosseini, E. Babaei, and J. Ebrahimi, "Interleaved high step-up dc-dc converter based on three-winding high-frequency coupled inductor and voltage multiplier cell," *IET Power Electron.,* Vol. 8, No. 2, pp. 175-189, Feb. 2015.
[18] L. Po-Wa, Y. S. Lee, D. K. W. Cheng, and L. Xiu-Cheng, "Steady-state analysis of an interleaved boost converter with coupled inductors," *IEEE Trans. Ind. Electron.,* Vol. 47, No. 4, pp. 787-795, Aug. 2000.
[19] Y. Ye, K. W. E. Cheng, and S. Chen, "A high step-up PWM DC-DC converter with coupled-inductor and resonant switched-capacitor," *IEEE Trans. Power Electron.,* Vol. 32, No. 10, pp. 7739-7749, Nov. 2016.
[20] F. H. Khan, L. M. Tolbert, and W. E. Webb, "Start-up and dynamic modeling of the multilevel modular capacitor-clamped converter," *IEEE Trans. Power Electron.,* Vol. 25, No. 2, pp. 519-531, Feb. 2010.
[21] F. H. Khan, L. M. Tolbert, and W. E. Webb, "Hybird electric vehicle power management solutions based on isolated and nonisolated configurations of multilevel modular capacitor-clamped converter," *IEEE Trans. Ind. Electron.,* Vol. 56, No. 8, pp. 3079-3095, May 2009.
[22] D. Cao, S. Jiang, and F. Z. Peng, "Optimal design of a multilevel modular capacitor-clampled DC-DC converter," *IEEE Trans. Power Electron.,* Vol. 28, No. 8, pp. 3816-3826, Aug. 2013.
[23] F. H. Khan and L. M. Tolbert, "Multiple-load-source integration in a multilevel modular capacitor-clamped DC-DC converter featuring fault tolerant capability," *IEEE Trans. Power Electron.,* Vol. 24, No. 1, pp. 14-24, Jan. 2009.
[24] L. Sun, F. Zhuo, F. Wang, and T. Zhu, "A non-isolated bidirectional soft-switching power-unit-based DC-DC converter with unipolar and bipolar structure for DC networks interconnection," *IEEE Trans. Ind. Appl*., Vol. 54, No. 3, pp. 2677-2689, Jan. 2018.

**Lejia Sun** received his B.S. degree in Electrical Engineering from Northwestern Polytechnical University (NPU), Xi'an China, in 2008. He received his M.S. and Ph.D. degrees in Electrical Engineering from Xi'an Jiaotong University (XJTU), Xi'an, China. In 2011, he joined the STATE GRIDS Corporation of China, and worked as the Project Manager. He was placed in charge of some national key projects related to ultra-high voltage (UHV) transmission (e.g: he worked as the Project Manager of the 1000kV EHV Yu Heng transformer substation and the ±800kV EHVDC Shan Bei converter station, in 2015 and 2017, respectively). He is presently working in the UHV Transmission Technology Research Department of the STATE GRIDS Corporation of China. His current research interests include power electronics, HVDC, DC/DC conversion, and distributed power systems. Professor Sun is also with the State Key Laboratory of Electrical Insulation and Power Equipment at XJTU.

**Fang Zhuo** was born in Shanghai, China, in 1962. He received his B.S., M.S. and Ph.D. degrees in Automatic Control and Electrical Engineering from Xi'an Jiaotong University (XJTU), Xi'an, China, in 1984, 1989 and 2001, respectively. He is presently working as a Ph.D. Supervisor at XJTU. He was the key finisher of four projects sponsored by the National Natural Science Foundation of China. He received four provincial and ministerial level science and technology advancement awards. He is the Power Quality Professional Chairman of the Power Supply Society of China. His current research interests include power quality, active power filters, reactive power compensation and distributed power generation.

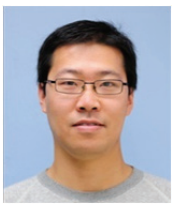

**Feng Wang** received his B.S., M.S. and Ph.D. degrees in Electrical Engineering from Xi'an Jiaotong University (XJTU), Xi'an China, in 2005, 2009 and 2013, respectively. From November 2010 to November 2012, he was an Exchanging Ph.D. student in the Center for Power Electronics Systems (CPES) at the Virginia Polytechnic Institute and State University, Blacksburg, VA, USA. In November 2013, he joined XJTU as a Postdoctoral Fellow. He is presently working as an Associate Professor at XJTU. His current research interests include DC/DC conversion and high power converters, especially in renewable energy generation fields.

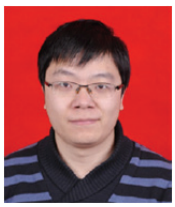

**Hao Yi** received his M.S. and Ph.D. degrees in Electrical Engineering from Xi'an Jiaotong University, Xi'an, China, in 2010 and 2013, respectively. Since 2013, he has been a Member of School of Electrical Engineering at Xi'an Jiaotong University. His current research interests include the modeling and control of high-power converters, the control and power management of microgrids, and power quality improvement.